Chapter 4

1,3-Dihydroxyacetone

4.1 Introduction

One of the sugars detected in carbonaceous chondrites is 1,3-dihydroxyacetone, or $CO(CH_2OH)_2$. Dihydroxyacetone is a monosaccharide commonly used as the active ingredient in sunless tanning products. Monosaccharides are polyhydroxylated aldehydes (or aldoses, whose chemical formula is $H\text{-}[CHOH]_k\text{-}CHO$) and ketones (or ketoses, whose general structure is given by $H\text{-}[CHOH]_l\text{-}CO\text{-}[CHOH]_m\text{-}H$) with the general formula $[C(H_2O)]_n$, where $n \geq 3$. Dihydroxyacetone and glyceraldehyde ($CH_2OHCHOHCHO$) are thus the simplest ketose and aldose monosaccharides, respectively. Dihydroxyacetone is used in numerous biological pathways, including the production of ATP, and is synthesized via glycolysis.

The 2C species glycolaldehyde is less stable than its structural isomers acetic acid (CH_3COOH) and methyl formate ($HCOOCH_3$), with methyl formate being the most stable. Similar patterns are observed with the 3C analogs, with sugars being more energetic than esters and acids (hence their biological utility), while ketoses are more stable than aldoses. The relative energies for the 2C and 3C structural isomers were calculated from Gaussian 98 MP2 6-311G++(d,p) geometry optimizations [31], and these results are discussed in

Appendix D.

The relative energies of the 3C sugars indicate that dihydroxyacetone would be more likely to survive under hot core conditions than glyceraldehyde. Indeed, in the laboratory glyceraldehyde is seen to isomerize to dihydroxyacetone [32]. Lovas et al. recently characterized the rotational spectrum of dihydroxyacetone to 40 GHz, fitting rotational and quartic centrifugal distortion constants to FTMW data [32]. We simultaneously began our study of dihydroxyacetone in a similar manner, using *ab initio* studies to guide initial FTMW experiments to 18 GHz. We then conducted millimeter and submillimeter direct absorption experiments to provide more accurate spectral predictions for observational searches.

The laboratory studies of glyceraldehyde and dihydroxyacetone provided the necessary basis for deep observational studies [32, 33]. The C_{2v} symmetry of dihydroxyacetone leads to somewhat stronger millimeter-wave emission features compared to glyceraldehyde. A glyceraldehyde K-band search with the GBT to an RMS of ~5 mK revealed no transitions [17].

The *ab initio* studies of dihydroxyacetone are presented in Section 4.2, while the laboratory studies of dihydroxyacetone are presented in Section 4.3. The results of observational searches for dihydroxyacetone are given in Section 4.4.

4.2   *Ab Initio* Studies

Quantum mechanical calculations were utilized to aid in spectral predictions for dihydroxyacetone. These calculations used B3LYP Density Functional Theory (DFT) [34, 35] and were performed in two phases. The first phase used a fairly small basis set and level of theory to delineate geometries with low energies. The second phase performed

more precise quantum mechanical calculations with the best geometries from the first phase. Calculations were performed using Jaguar version 4.2, release 77 [36].

During the first phase of the calculations, the 6-31G basis set was used [37]. The four angular degrees of freedom for dihydroxyacetone were constrained to be multiples of 60 degrees while all other degrees of freedom were optimized. From these optimized geometries, the 5% with the lowest energy were used in the second phase. Here, all degrees of freedom were optimized, and the 6-31G**++ basis set was used [37–39]. Separate conformers were distinguishable by unique values for the dipole moments, and roughly ten possible geometries were optimized for each of the lowest four conformers. The rotational constants determined for each conformer were then averaged across all geometries. Relative energies, dipole moments, and rotational constants determined for the two lowest energy conformers (see Table 4.1) were then used for initial spectral predictions. The structures of these two conformers are shown in Figure 4.1. The ground state conformer optimized geometry is included in the analysis of Lovas et al. [32] and is of C_{2v} symmetry. The non-zero μ_a and μ_c values obtained in our study for this conformer are therefore unexpected and are likely artifacts of the averaging approach used for determination of each structure's parameters. Indeed, Lovas et al. report only a b-type dipole moment [32]. The higher energy conformer structural parameters have not been included because of the rather large inherent uncertainty due to this averaging approach as well as the unlikeliness of this conformer to exist under normal laboratory or interstellar conditions.

Table 4.1: Spectral parameters predicted for dihydroxyacetone from quantum mechanical calculations using B3LYP DFT.

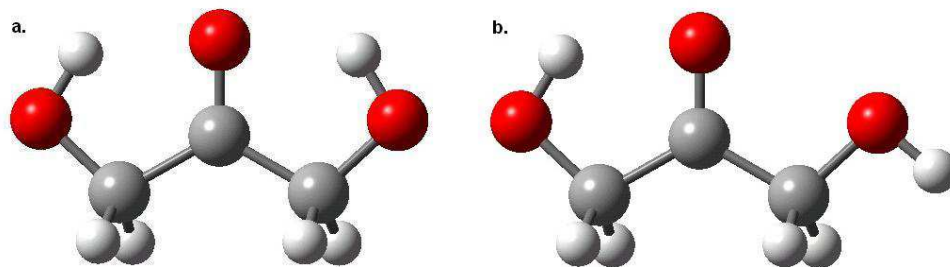| Parameter	Conformer 1	Conformer 2
E	0 kcal/mol	1.9214 kcal/mol
A	9862.419 MHz	5942.059 MHz
B	2035.671 MHz	2656.905 MHz
C	1724.558 MHz	1787.788 MHz
μ_a	0.007 D	2.150 D
μ_b	1.859 D	3.601 D
μ_c	0.019 D	0.036 D

Figure 4.1: Structures of the two lowest energy dihydroxyacetone conformers: a. doubly hydrogen bonded conformer (ground state); b. singly hydrogen bonded conformer.

4.3 Spectroscopic Studies

4.3.1 Experimental

All experiments were conducted with dihydroxyacetone vapor from a sample of solid 1,3-dihydroxyacetone dimer (97% purity) purchased from Aldrich.

4.3.2 FT-Microwave Studies

The FTMW experiments were conducted with the original Balle-Flygare spectrometer. The details of the setup can be found in Chapter 2, Appendix A, and reference [20]. A

sample holder containing solid dihydroxyacetone was placed after the pulsed valve and heated sufficiently to obtain a dihydroxyacetone vapor pressure of ~ 1 Torr. Argon gas was pulsed over the sample, and a molecular beam was formed by a Laval nozzle at the exit of the heated compartment (see reference [21] for further details on the heated nozzle). Predictions based on the theoretical calculations were used to guide spectral line searches. Four ^{b}R and one ^{b}Q transition were chosen for these initial searches based on their predicted line strengths. Once the $1_{0,0} \rightarrow 0_{0,0}$ transition was observed, the single-shot signal was optimized before additional spectral searches were conducted. The instrument was used in the coaxial valve configuration, resulting in classic Doppler doublets for all transitions. Linewidths were on the order of 8 kHz (see Figure 4.2). Additional searches for the singly H-bonded conformer were conducted, but no lines were observed in the supersonic expansion.
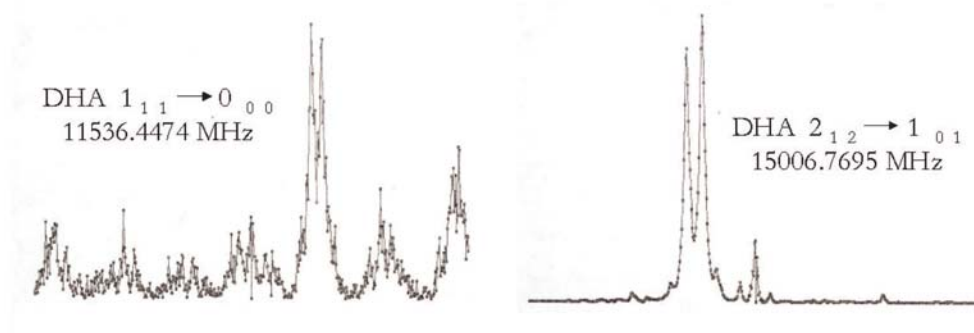

Figure 4.2: Single-shot dihydroxyacetone spectra from the FT-microwave experiments.

4.3.3 Direct Absorption Millimeter and Submillimeter Studies

Studies were conducted with the 3 mm Caltech Direct Absorption Flow Cell Spectrometer. The details of the setup can be found in Chapter 2, Appendix B, and reference [40]. Computer-automated scans of both increasing and decreasing frequency

increments were averaged in areas of low power to increase the signal-to-noise ratio. This averaging was not required for all scans as the frequency shifts due to the time constant of the lock-in amplifier were smaller than the spectral resolution. The solid dihydroxyacetone sample was placed directly in the cell, and heating tape was wrapped around this section of the cell and used to gently heat the sample to approximately 50 °C. A pressure of approximately 100 mtorr was maintained for the duration of the experiment.

An example spectrum from 112–120 GHz is shown in Figure 4.3. Strong ^bR branches are seen at a separation of approximately 4 GHz. Linewidths were on the order of 1 MHz.
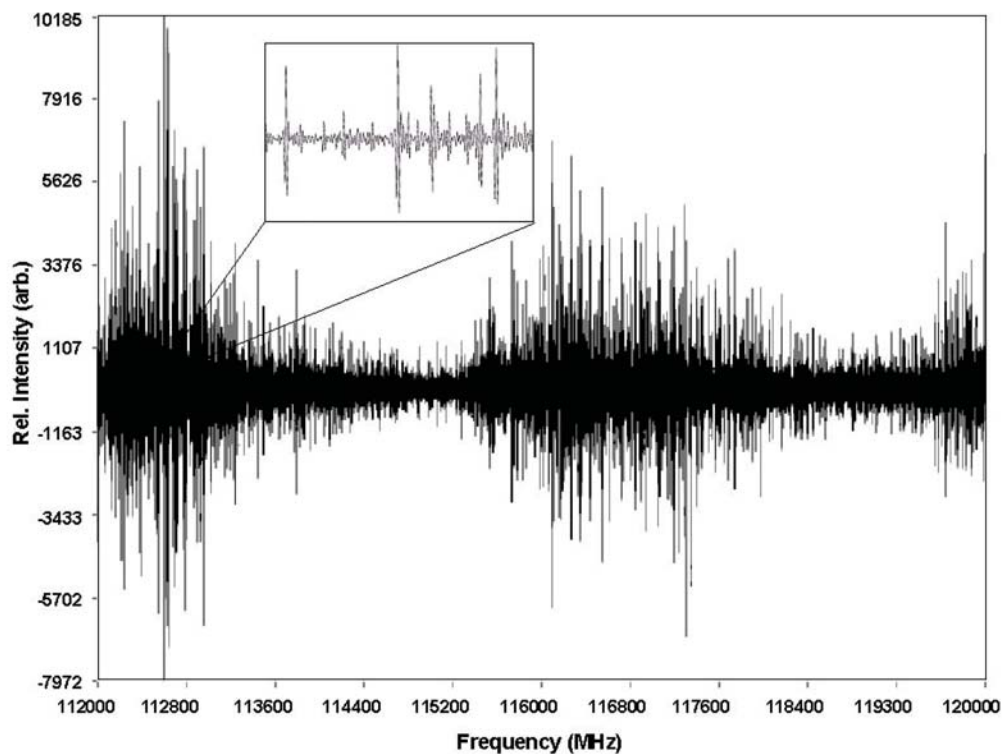

Figure 4.3: The flow cell dihydroxyacetone spectrum from 112 to 120 GHz.

The higher frequency (sub)millimeter studies were conducted with the JPL flow cell

spectrometer. The basic flow cell design and detection methods for the JPL spectrometer are outlined in reference [23]. The source frequencies were obtained using a directly synthesized beam projected from the output of a multiplier chain [41]. Second and third harmonics of this multiplier were produced on a whisker-contacted Schottky diode and detected with a helium cooled InSb bolometer. Again, averaging was not required as the errors due to the time constant of the lock-in amplifier were smaller than the spectral resolution. Linewidths were of order 1 MHz. No sample heating was required for these experiments because of the strength of the submillimeter lines. A pressure of approximately 10 mtorr was maintained for the duration of the experiment.

4.3.4   Data Analysis

The data were assigned using the SPFIT and SPCAT programs (see Appendix C, [30]). The rotational constants obtained with the *ab initio* studies, the dipole moments from reference [32], and a standard asymmetric-top Hamiltonian with the Watson A-reduction were used to generate a predicted spectrum. The initial microwave data were used to fit the rotational constants and estimate the quartic distortion constants. These constants were then used to predict the millimeter spectrum. As new data were assigned, lines were continuously added to the data set and the spectral fit further modified with the same asymmetric-top Hamiltonian. The quality of the fit to the entire data set was indicated by a microwave root mean square deviation.

A total of 2360 dihydroxyacetone lines were assigned. Significant harmonic contamination was present in the submillimeter scans, but the presence of acetonitrile as a cell contaminant led to accurate determination of the frequencies within spectral regions where acetonitrile lines were observed. However, this contaminant also led to line confusion

for weaker dihydroxyacetone lines. Therefore, while approximately 95% of the 2σ lines were assigned in the millimeter spectrum, only the strongest lines ($\sim$75% of the total lines) were assigned in the submillimeter spectra. These submillimeter assignments include almost all strong ground state transitions as well as the strongest R and Q type transitions for the other vibrational states.

Only the ground state assignments were made initially, with quartic centrifugal distortion constants determined in addition to the standard rotational constants. A total of 1284 lines have been assigned to the ground state with an RMS of 98 kHz. Additional assignments were made for four vibrational states, with RMS values ranging from 99 to 268 kHz. Although decreasing the pressure during the millimeter and submillimeter experiments could have resulted in narrower lines and therefore a lower RMS, this would have significantly decreased the observed signal and made spectral assignment quite difficult. The files associated with the analysis, including the parameters and rest frequencies, can be found in Appendix E. The output file from the spectral analysis, which includes the observed minus calculated residuals, has been included as supplementary material in the electronic version of this thesis. The assignments and other predicted rotational frequencies are accessible through the submillimeter and microwave spectral line catalog available at `http://spec.jpl.nasa.gov` [30]. The rotational and centrifugal distortion constants determined for each state are listed in Table 4.2.

As no vibrational spectral studies have been conducted for the torsional states of dihydroxyacetone, assignments of the vibrational state energies were based on the relative intensities of the observed lines to those from the ground state. Approximate relative energies were determined for each vibrational state and are included in Table 4.2. The rotational and quartic centrifugal distortion constants were determined independently for

Table 4.2: Spectral parameters determined for dihydroxyacetone.

state	ν_0	ν_1	ν_2	
E	0	~93	~147	cm^{-1}
A	9801.294341(269)	9764.48006(113)	9701.67778(178)	MHz
B	2051.525611(76)	2049.846696(274)	2051.55037(42)	MHz
C	1735.164871(77)	1736.322262(248)	1737.92899(33)	MHz
Δ_J	0.1823699(94)	0.183278(33)	0.185158(62)	kHz
Δ_{JK}	0.657039(88)	0.84847(40)	0.50245(102)	kHz
Δ_K	5.36670(50)	5.4775(57)	3.4799(110)	kHz
δ_J	0.02767300(181)	0.0274086(134)	0.0276239(291)	kHz
δ_K	0.569401(157)	0.64161(96)	0.35886(184)	kHz
# Lines	1284	490	312	
Fit RMS	0.098	0.099	0.142	MHz

state	ν_3	ν_4	
E	~150	~183	cm^{-1}
A	9662.11092(271)	10329.1(106)	MHz
B	2050.02151(45)	2065.17(41)	MHz
C	1739.41934(37)	1735.12347(60)	MHz
Δ_J	0.187123(60)		kHz
Δ_{JK}	0.60623(79)		kHz
Δ_K	7.1160(185)		kHz
δ_J	0.0265674(279)		kHz
δ_K	0.31951(205)		kHz
# Lines	241	34	
Fit RMS	0.178	0.268	

Note: One σ errors are listed in parentheses in units of last significant figure. The quartic distortion constants for the ground state were used for the fourth vibrational state.

three vibrational states. Only a partial fit has been completed for the highest energy vibrational state due to its relatively weak line strengths. In this case, the quartic distortion constants were held to the values determined for the ground state. The microwave RMS determined for this state is therefore considerably higher than those determined for the others.

4.3.5 Discussion

The millimeter and submillimeter spectra of dihydroxyacetone have been characterized up to 450 GHz. Spectral assignments include lines from the ground state and four vibrational states, and rotational and quartic centrifugal distortion constants have been determined for each of these states. Excluding the fourth vibrational state, predictions of strong submillimeter lines above 450 GHz are accurate to better than 1 MHz, and interpolations below 450 GHz are accurate to less than 100 kHz for all states based on this analysis.

The spectral parameters determined by quantum mechanical calculations were accurate to less than 1% of the experimentally determined values, indicating the value of density functional theory as a tool for the prediction of pure rotational spectra.

It was found, however, that millimeter and submillimeter predictions based on the initial FTMW work are not sufficiently accurate for observational searches in these ranges. Indeed, at 1.3 mm, near the peak of the Boltzmann distribution for dihydroxyacetone under typical hot core conditions, the microwave-based predictions for the strongest transitions differ by 10-15 MHz from the experimentally measured line positions. This corresponds to a velocity shift of >15 km/sec from the source velocity. Interstellar detection of this molecule would be quite difficult based on these parameters. Because of the relative rigidity of dihydroxyacetone in comparison to most complex organic species predicted to be present in hot cores, this study also indicates that further analysis of the rotational spectra of complex molecules beyond the microwave region is necessary to guide observational searches.

4.4   Observational Studies

The laboratory investigation of dihydroxyacetone provided the necessary information to guide observational searches using microwave through submillimeter wave telescopes. Searches for dihydroxyacetone were therefore conducted with the CSO, OVRO, and GBT observatories, and these observations are outlined below.

4.4.1   CSO Observations

4.4.1.1   Observations

A search for dihydroxyacetone emission in the 1.3 mm atmospheric window was conducted with the CSO. Initial searches were conducted toward the Sgr B2(N-LMH) hot core. The parameters for the dihydroxyacetone lines used in this search, specifically the transition quantum numbers, rest frequencies, Einstein A-coefficients times the upper state degeneracy, and upper state energies, are listed in Table 4.3. All observed lines are transitions within the ground vibrational state. Many of these lines are actually asymmetry doublets or blends of multiple transitions between similar yet distinct quantum states whose energies are nearly degenerate. These will appear in observational spectra as a single blended line because of the ~10 km s^{-1} linewidths characteristic of Sgr B2. Only one frequency has been listed for asymmetry doublets occurring at the same frequency; for all others, the frequency of each individual component has been listed.

The survey was conducted using the CSO 230 GHz double sideband (DSB) heterodyne receiver on the nights of 2003 July 13–23/September 14–21 and 2004 June 30–July 7. Typical system temperatures ranged from 200–600 K, and the source position selected was $\alpha(1950)=17^h\ 44^m\ 10^s.1$, $\delta(1950)=$ -28° 21′ 17″, which is coincident with the Sgr B2(N-LMH)

Table 4.3: A summary of dihydroxyacetone emission lines from Sgr B2(N-LMH).

$J'_{K'_a,K'_c}-J''_{K''_a,K''_c}$	ν_0^a (MHz)	$Ag_u\times10^2$ (s^{-1})	E_u (K)	T_{MB}^b (K)	Δv^c (km s^{-1})	v_{LSR}^c (km s^{-1})
$14_{11,3} \rightarrow 13_{10,4}$	219059.1	1.23	64.98	0.14	10.60(16)	62.91(17)
$14_{11,4} \rightarrow 13_{10,3}$		1.23	64.98			
$61_{3,58} \rightarrow 60_{4,57}$	222826.4	5.17	344.98	0.48	11.50(250)	64.50(21)
$61_{4,58} \rightarrow 60_{3,57}$	222839.4	5.71	344.98	0.39	7.74(224)	65.23(26)
$15_{11,4} \rightarrow 14_{10,5}$	222847.0	1.44	67.71	0.35	8.29(252)	60.74(40)
$15_{11,5} \rightarrow 14_{10,4}$		1.44	67.71			
$60_{5,56} \rightarrow 59_{4,55}$	222861.1	4.78	341.68	0.19	10.77(132)	63.24(42)
$63_{1,62} \rightarrow 62_{2,61}$	223293.9	6.78	349.60	0.40	17.36(64)	62.38(9)
$63_{2,62} \rightarrow 62_{1,61}$		6.78	349.60			
$67_{3,64} \rightarrow 66_{4,63}$	243591.0	8.53	412.61	0.24	13.12(51)	63.78(10)
$67_{4,64} \rightarrow 66_{3,63}$	243593.0	8.53	412.61			
$72_{1,71} \rightarrow 71_{2,70}$	254459.9	11.67	453.49	0.20	8.95(140)	65.86(19)
$72_{2,71} \rightarrow 71_{1,70}$		11.67	453.49			
$75_{0,75} \rightarrow 74_{1,74}$	261654.3	14.30	479.97	0.18	9.22(46)	62.31(12)
$75_{1,75} \rightarrow 74_{0,74}$		14.30	479.97			

[a] One σ uncertainties are 0.1 MHz.
[b] One σ uncertainties are <10 mK.
[c] One σ uncertainties are listed in parentheses in units of last significant figure.

hot core. The chopping secondary with a $70''$ throw was used along with chopper-wheel calibration and the facility 1.5 GHz, 500 MHz, and 50 MHz acousto-optic spectrometer (AOS) back ends to minimize the spectral baseline fluctuations. The FWHM of the CSO at these frequencies is $\sim30''$, and all data are placed on the T_{MB} temperature scale using a main beam efficiency of 70% determined using observations of the planets. Line confusion was a perpetual difficulty faced during the observations due to the DSB setup of the CSO and

the dense spectral line nature of the Sgr B2(N-LMH) source. Line positions were therefore verified by observing several small frequency offsets at each local oscillator (LO) setting. A v_{LSR} of 62 km/s was used for the July 2003 observations. Potential dihydroxyacetone lines were observed at 64 km/s, so this v_{LSR} was then used for the remaining observations.

Additional observations were conducted towards the Orion Compact Ridge and W51e2 hot core sources on the nights of 2003 September 14–21/December 14–16. The spectral windows centered at 222839 and 243591 MHz were observed in each source (see Table 4.3). Typical system temperatures ranged from 200-600 K, and the source positions and velocities used were $\alpha(2000)$=05^h 35^m 14^s.5, $\delta(2000)$= -05° 22′ 30″.4 and 9 km/s for the Orion Compact Ridge, and $\alpha(1950)$=19^h 23^m 43^s.5, $\delta(1950)$= 14° 30′ 34″ and 55 km/s for the W51e2 hot core. The observing parameters outlined above for the Sgr B2 search were also used for these observations.

4.4.1.2 Results

A total of nine possible dihydroxyacetone emission lines were detected in Sgr B2(N-LMH) with the CSO. The mean v_{LSR} is 63.4 ± 3.2 km/s. The observational spectra from the 500 MHz AOS in the v_{LSR} = 0 - 100 km/s window are shown in Figure 4.4. The v_{LSR} scales have been adjusted such that the LO frequency is centered at 64 km/s. Nine additional lines were either severely blended with other lines or completely obscured by stronger features in the signal or image sideband. No dihydroxyacetone lines were found to be absent in this source from any clean 1.3 mm spectral windows observable at the CSO.

Least-squares Gaussian fits to each observed line are summarized in Table 4.3 and shown in Figure 4.4. The integrated intensity was calculated by Equation 3.2, where T_{MB} = T_A^*/0.7 for the CSO at 230 GHz. No beam dilution corrections were applied because the
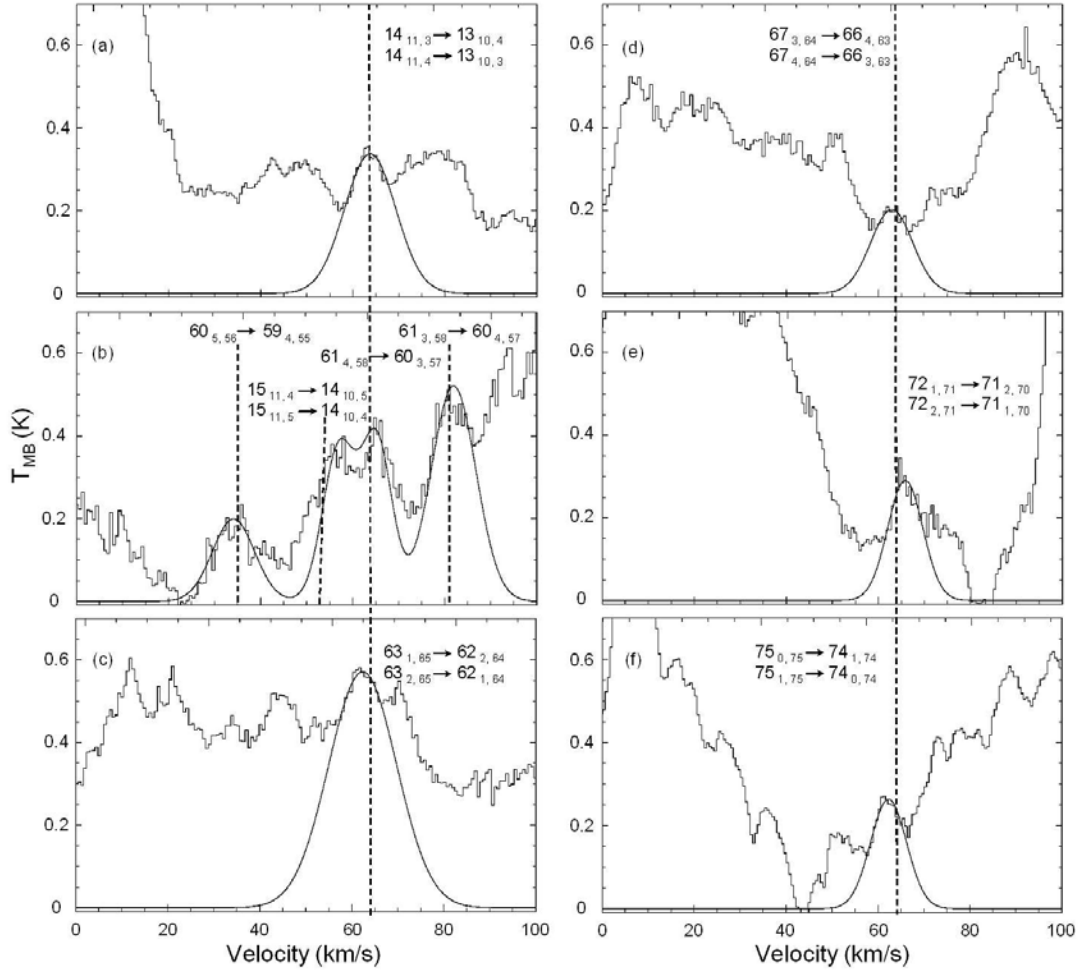
Figure 4.4: Possible dihydroxyacetone transitions observed toward Sgr B2(N-LMH) with the least-squares Gaussian fits to each line. Spectra are from the CSO 500 MHz AOS, and a linear baseline subtraction of the continuum has been performed. The vertical dotted line indicates $v_{lsr} = 64$ km/s. The positions of additional dihydroxyacetone lines relative to 64 km/s are indicated in spectrum (b).

spatial scale of the emission is unknown. Only single Gaussian fits are reported here since many of the potentially blended lines in Figure 4.4 are unassigned, and hence the relative contributions from individual features are poorly constrained.

A rotation diagram approach was used to determine the rotational temperature and

column density of dihydroxyacetone toward SgrB2(N-LMH) (see Section 3.3). Only the ground and first four dihydroxyacetone vibrational states are populated at $T \sim 250$ K, and a full rotational analysis has been performed for these states (see Section 4.3 and reference [33]). The rotational constants determined for each vibrational state have therefore been used such that the partition function is approximated as:

$$Q(T_{rot}) \approx \sum_{i=0}^{4} e^{-E_i/kT_{rot}} \sqrt{\frac{\pi}{A_i B_i C_i} \left(\frac{kT_{rot}}{h}\right)^3} \qquad (4.1)$$

The rotation diagram for dihydroxyacetone is shown in Figure 4.5. A molecular rotational temperature of 222 ± 65 K and a column density of $(4.9 \pm 2.2) \times 10^{15}$ cm^{-2} were derived, where the errors represent 95% confidence intervals.

Four lines corresponding to dihydroxyacetone transitions were observed in one window at the 222839.40 MHz LO setting (Figure 4.4b); these data are shown in Figure 4.6 along with a T_{rot}=220 K simulated spectrum. The relative intensities, line center frequencies, and linewidths of the dihydroxyacetone lines were fixed and the intensities scaled to best match the observed spectrum. The additional strong line is due to H$_2^{13}$CO in the image sideband, and all parameters for this line were fixed to those determined in reference [24]. The simulation shows that other unidentified spectral features may be present in the DSB spectrum, and that the integrated intensity of the 222826.4 MHz dihydroxyacetone line is most affected by these features. It is therefore not included in the rotation diagram analysis.

A spectral window overlapping in frequency with two strong dihydroxyacetone lines has also been observed in this source with the Kitt Peak 12 meter telescope (J. M. Hollis 2004, private communication). There are emission features at the appropriate frequencies for these dihydroxyacetone transitions but one of the lines appears to be blended with an
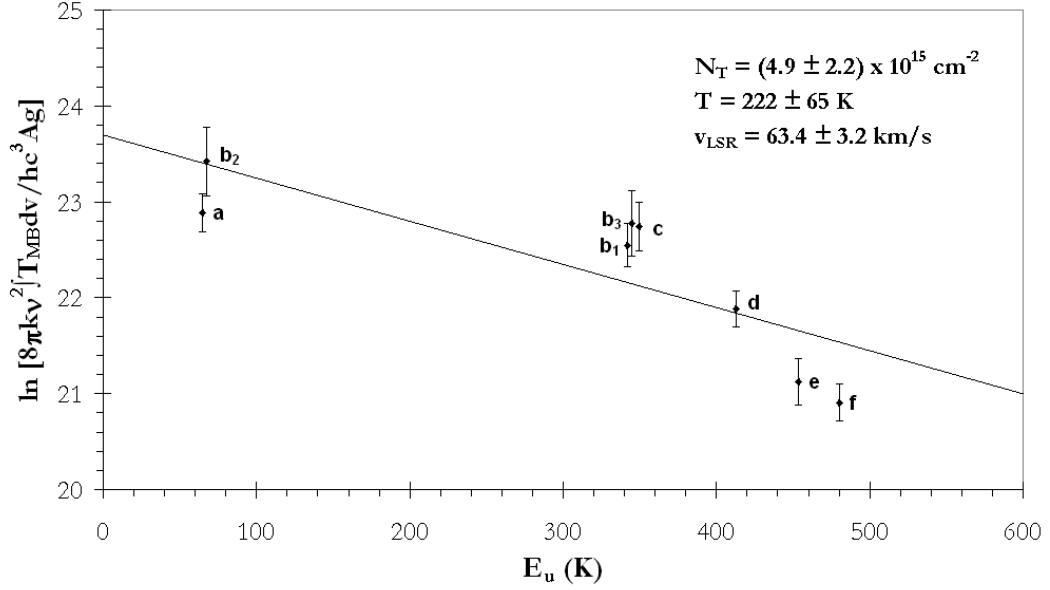
Figure 4.5: The rotation diagram for dihydroxyacetone toward SgrB2(N-LMH). The labels correspond to the panels of Figure 4.4.

unidentified line. Their inclusion in the rotation diagram analysis is quite difficult due to the lack of information regarding linewidths for dihydroxyacetone emission features in this frequency range, and therefore these data have not been included in this study.

No transitions were observed toward the Orion or W51 hot cores, and so the column density upper limit was calculated from the observed spectral intensity at the expected line position, which was placed on the T_{MB} temperature scale using a main beam efficiency of 70%. These limits are presented in Table 4.4. A linewidth of 5 km/s and a rotational temperature of 150 K, typical values observed for species in the Compact Ridge, were assumed for the Orion calculations [25]. A line width of 10 km/s and a rotational temperature of 100 K, the values found for methyl cyanide in the W51e2 source, were assumed for the W51e2 calculations [42].
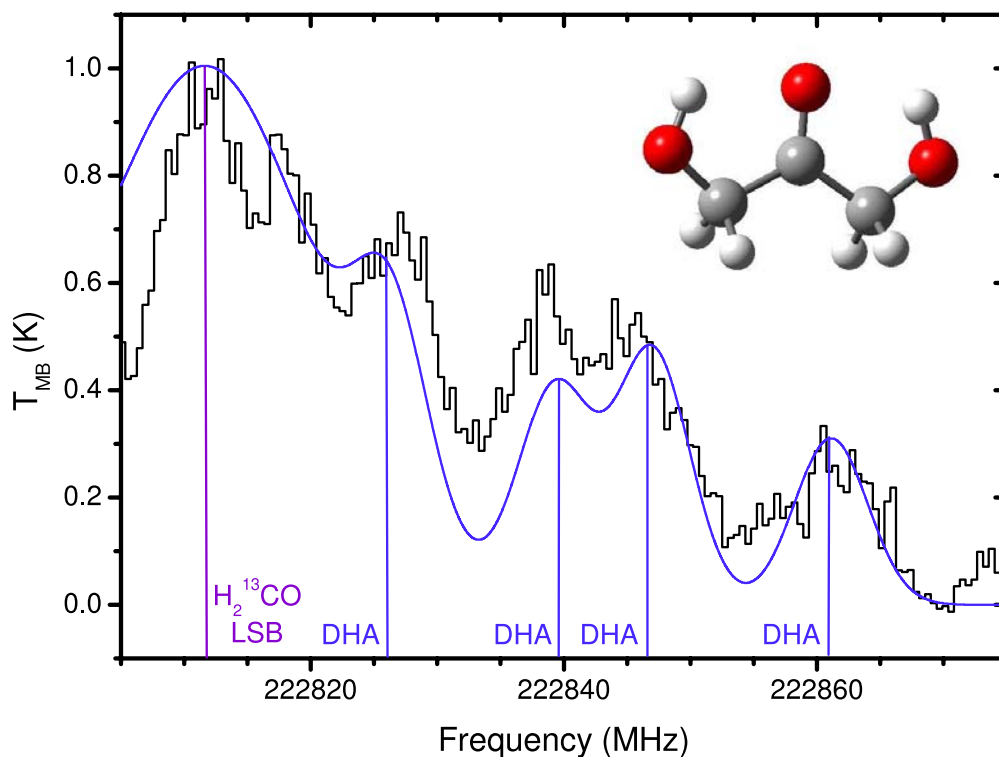
Figure 4.6: The simulated spectrum of dihydroxyacetone lines at 220 K compared to an observed Sgr B2(N-LMH) spectrum. The structure of dihydroxyacetone is shown in the inset.

4.4.2 OVRO Observations

4.4.2.1 Observations

Observations to image potential dihydroxyacetone emission in the Sgr B2(N-LMH) source were conducted with the OVRO Millimeter Array between 2003 October 13–November 18 and 2004 March 14–April 28. A source position of $\alpha(2000)$=17^h 47^m $19^s.92$, $\delta(2000)$= -28° 22′ 19″.5 served as the phase center, and all correlator modules were set up using a v_{LSR} of 64 km/s. These observations were conducted in the L and E configurations, resulting in a synthesized beam of 7″.9 × 4″.0 using robust weighting. The source was observed for

Table 4.4: Dihydroxyacetone column density upper limits in Orion and W51 from CSO observations.

$J'_{K'_a,K'_c}-J''_{K''_a,K''_c}$	ν_0^a (MHz)	$Ag_u\times10^2$ (s^{-1})	E_u (K)	T^b_{MB} (K)	N_T upper limit [c] ($\times10^{-13}$ cm^{-2})
Orion					
$61_{4,58}\rightarrow60_{3,57}$	222839.4	5.71	344.98	0.005(2)	0.98(14)
$67_{3,64}\rightarrow66_{4,63}$	243591.0	8.53	412.61	0.24(2)	18.7(28)
$67_{4,64}\rightarrow66_{3,63}$	243593.0	8.53	412.61		
W51e2					
$61_{4,58}\rightarrow60_{3,57}$	222839.4	5.71	344.98	0.065(2)	5.25(234)
$67_{3,64}\rightarrow66_{4,63}$	243591.0	8.53	412.61	0.12(2)	3.87(255)
$67_{4,64}\rightarrow66_{3,63}$	243593.0	8.53	412.61		

[a] One σ uncertainties are 0.1 MHz.
[b] Assumed uncertainties are listed in parentheses in units of last significant figure.
[c] One σ uncertainties are listed in parentheses in units of last significant figure.

approximately 5 hours in each full track, and 2.5 tracks were completed in L configuration, while 4 full tracks were completed in E configuration. Four dihydroxyacetone lines were observed simultaneously, and the parameters for these lines, specifically the transition quantum numbers, rest frequencies, Einstein A-coefficients times the upper state degeneracy, and upper state energies, are listed in Table 4.5. All observed lines are transitions within the ground vibrational state.

The quasars 3C345 and 3C454.3 were observed for secondary flux and bandpass calibration, with observations of Neptune and Uranus serving to bootstrap the quasar fluxes. Observations of phase and amplitude calibrators were conducted in approximately half hour integrals throughout the tracks. Baseline-based boxcar fits to an internal noise

source modified by a second order polynomial fit to observations of the quasars were used to derive the bandpass calibration. Bandpass, phase, and flux calibrations were applied to the data with the MMA software package [43]. The MIRIAD data reduction software package [44] was used for subsequent spectral analysis.

4.4.2.2 Results

None of the transitions were detected toward Sgr B2(N-LMH), and so the column density upper limit was calculated from the observed spectral intensity at the expected line position. The transition at 112.636609 GHz is near the edge of a strong spectral line from another species. This strong feature also makes spectral baseline determination quite difficult. The combination of these two factors greatly effects the observed intensity for this transition. A linewidth of 10 km/s, roughly the average linewidth observed in the CSO observations, was assumed for the upper limit calculations. The calculated dihydroxyacetone column density upper limits are presented in Table 4.5.

4.4.3 GBT Observations

4.4.3.1 Observations

Additional observations of low energy dihydroxyacetone transitions in the Sgr B2(N-LMH) source were conducted with the GBT on the night of 2005 April 5. A source position of $\alpha(2000)=17^h\ 47^m\ 19^s.92$, $\delta(2000)=$ -28° 22′ 19″.5 and a source velocity of 64 km/s were used. These observations were conducted with the Q-band receiver, which operates over the 40–52 GHz range. The GBT spectrometer back end was used in the 4 intermediate frequency (IF), 50 MHz bandwidth, 9 level mode that allows for four 50 MHz spectral windows to be observed simultaneously in dual polarization. The observations were conducted in position

Table 4.5: Dihydroxyacetone column density upper limits in Sgr B2(N-LMH) from OVRO observations.

$J'_{K'_a,K'_c} - J''_{K''_a,K''_c}$	ν_0^a (MHz)	$Ag_u \times 10^2$ (s^{-1})	E_u (K)	T_{MB}^b (K)	N_T upper limit [c] ($\times 10^{-15}$ cm^{-2})
$31_{2,30} \rightarrow 30_{1,29}$	112558.8289	0.3611	89.27	0.79(10)	14.2(44)
$42_{8,35} \rightarrow 42_{7,36}$	112612.4493	0.2095	291.30	0.34(7)	10.4(33)
$32_{0,32} \rightarrow 32_{1,31}$	112630.7384	0.4622	90.28	0.15(6)	2.14(66)
$32_{1,32} \rightarrow 31_{0,31}$	112636.6087	0.4624	90.28	0.12(6)	1.71(53)

[a] One σ uncertainties are 0.1 MHz.
[b] Uncertainties are listed in parentheses in units of last significant figure and are based on an assumed flux uncertainty of ± 0.02 Jy/Beam.
[c] One σ uncertainties are listed in parentheses in units of last significant figure.

switching mode, and a total of 3 hours of on-source integration was completed. The FWHM of the GBT at these frequencies is $\sim 16''$, and all data are placed on the T_{MB} temperature scale using a main beam efficiency of 40%. The parameters for the dihydroxyacetone lines in these windows, specifically the transition quantum numbers, rest frequencies, Einstein A-coefficients times the upper state degeneracy, and upper state energies, are listed in Table 4.6. All observed lines are transitions within the ground vibrational state.

4.4.3.2 Results

The data from each polarization of each IF setting were calibrated and co-added independently. The two polarizations in a given IF setting were then averaged to further reduce the RMS. The column density derived from the CSO observations indicates that an RMS level of ~ 5 mK (on the T_A^* scale) is required to ensure $>2\sigma$ detections for the dihydroxyacetone emission features in this spectral region. The minimum RMS level reached

Table 4.6: Dihydroxyacetone column density upper limits in Sgr B2(N-LMH) from GBT observations.

$J'_{K'_a,K'_c}-J''_{K''_a,K''_c}$	ν_0^a (MHz)	$Ag_u\times10^2$ (s^{-1})	E_u (K)	T^b_{MB} (K)	N_T upper limit [c] ($\times10^{-15}$ cm^{-2})
$30_{4,26} \rightarrow 30_{3,27}$	42007.7536	0.0071	13.79	0.025(8)	3.12(95)
$11_{1,11} \rightarrow 10_{0,10}$	41953.1665	0.0066	11.80	0.140(35)	19.1(582)
$12_{0,12} \rightarrow 11_{1,11}$	41525.1729	0.0058	20.00	0.033(10)	5.20(158)
$13_{3,11} \rightarrow 13_{2,12}$	42619.6200	0.0193	92.24	0.065(17)	3.05(94)

[a] One σ uncertainties are 0.1 MHz.
[b] Uncertainties are listed in parentheses in units of last significant figure and are based on an assumed flux uncertainty of ±0.02 Jy/Beam.
[c] One σ uncertainties are listed in parentheses in units of last significant figure.

in any of the 4 IF settings was on the order of 10 mK, and so none of the transitions were unambiguously observed. Emission is indeed seen at the dihydroxyacetone line positions, but the limited sensitivity of the observations combined with possible line confusion excludes the possibility for a definitive detection at this time. The column density upper limits were calculated from the observed spectral intensity at the expected line position. A linewidth of 10 km/s, roughly the average linewidth observed in the CSO observations, and the rotational temperature of 220 K determined from the CSO observations were assumed. The calculated dihydroxyacetone column density upper limits are presented in Table 4.6.

4.4.4 Discussion

The CSO Sgr B2 results are the first observational evidence for the presence of the 3C ketose 1,3-dihydroxyacetone in the ISM. The derived dihydroxyacetone excitation and velocity are in excellent agreement with other species detected in the Sgr B2(N-LMH) hot core, for which the most commonly quoted rotational temperature and v_{LSR} are 200 K and 64 km s^{-1}, respectively (see [28] and references therein).

The absence of dihydroxyacetone lines in the OVRO spectra does not further substantiate the CSO observations. The limits derived from these observations, however, are on the same order as or greater than the column density determined from the CSO observations and therefore do not rule out the possibility of dihydroxyacetone being present in this source if the emission is extended. The OVRO observations would be the least affected by beam dilution should the emission be compact, and so these results provide the upper limit to the column density in this case. More sensitive observations are required for determining the spatial scale of dihydroxyacetone emission in this source, and the Combined Array for Millimeter Astronomy (CARMA), which will be commissioned in 2006, will be used for this study.

Other molecules observed in Sgr B2(N-LMH) show two-component behavior in which higher energy transitions give characteristic hot core temperatures, but lower energy transitions yield much colder excitation temperatures. It is thought that these lower energy states are populated in an extended, potentially subthermally excited, source, possibly formed by shock liberated grain mantle ices [17,18]. Dihydroxyacetone should demonstrate such behavior if it is produced by grain surface chemistry. Unfortunately the sensitivity levels reached in the GBT observations remain insufficient for a definitive detection of this type of low-energy emission. The GBT and CSO observations are directly comparable for

a source size larger than $30''$, and the GBT limits lie well within the margin of error for the column density derived from the CSO observations. A source size on the order of $10''$, such as that observed for ethyl cyanide in this source [45], requires that these results be scaled appropriately to account for beam dilution effects. This results in a column density limit from the GBT observations of $1.09(34) \times 10^{15}$ cm^{-2}, indicating that the line confusion in the CSO observations may be leading to an overestimation of the column density by approximately a factor of four if the source is on the order of $10''$ in size.

The dihydroxyacetone lines observed in the Sgr B2(N-LMH) source are not present in the Orion and W51e2 spectra obtained with the CSO. The limits derived from these observations put constraints on the sugar-related chemistry in these sources. The absence of these spectral features also further strengthens the detection of dihydroxyacetone in Sgr B2(N-LMH). It is possible that weak spectral features in hot core sources may be due to unidentified vibrationally excited lines of a simpler, previously detected hot core molecule. It is clear that these emission features are not due to such a transition if they are present only in the Sgr B2(N-LMH) hot core.

The derived dihydroxyacetone column density of $(4.9 \pm 2.2) \times 10^{15}$ cm^{-2} leads to interesting questions about the formation of and subsequent behavior of this molecule in the hot core. Emission from the high excitation lines of methyl formate, acetic acid, ethyl cyanide (CH_3CH_2CN), dimethyl ether (CH_3OCH_3), and acetone (($CH_3)_2CO$) is known to be compact with respect to the CSO beam (see [46] and references therein). If similar filling factors are used for dihydroxyacetone then it would be more abundant than any of these compounds except dimethyl ether. Even if the column density derived from the CSO observations is overestimated by a factor of four, dihydroxyacetone would still be present at similar abundances to these species. Both the chopping scheme and higher frequencies of

CSO observations render them insensitive to spatial distribution for extended, low excitation emission as is seen from molecules such as acetaldehyde, ethanol, and glycolaldehyde. Direct comparisons show that these molecules are also less abundant than dihydroxyacetone.

A further complication is the inconsistent treatment of the partition functions of complex molecules. Typically only the ground vibrational state is included in partition function calculations as laboratory characterizations of excited states are often incomplete. Inclusion of vibrational state terms can greatly effect the derived total column densities of complex species under hot core conditions. For a molecule like glycolaldehyde, the inclusion of torsional states increases the partition function by $\sim$50% at 200 K, but they can be safely ignored below 50 K (see Chapter 6 and reference [47]). Exclusion of excited vibrational state terms in the dihydroxyacetone analysis would lower the column density by $\sim$60%.

Nevertheless, dihydroxyacetone would be among the most abundant complex molecules in the Sgr B2(N-LMH) hot core should the present analysis be confirmed by further observations, and so an efficient formation route must exist. No quantitative chemical scheme for the production of species such as glycolaldehyde and dihydroxyacetone has been presented. Observations of complex molecules toward low mass protostars where the dynamical time scales are short [2, 48] and careful studies of the potential reactions leading to methyl formate all seem to point toward a grain mantle synthesis [13]. In this regard it is intriguing to note that, with appropriate rearrangements, all of these species can be formed from reactions involving the abundant grain mantle constituents CO, HCOOH, and CH_3OH or their radical precursors. The importance of such reactions in interstellar grain surface chemistry is discussed in Chapter 8.

Survivability in hot cores may be another important aspect of dihydroxyacetone chemistry. As a ketose, it is both thermodynamically more stable and less reactive than

either glycolaldehyde or glyceraldehyde in hot gas. Isomerism in 3C and larger compounds is also quite extensive, and both dimethyl carbonate ($(CH_3O)_2CO$) and methyl glycolate (CH_3OCOCH_2OH) are even more stable than dihydroxyacetone. These isomers would likely be created by any surface chemistry leading to sugars. Laboratory and observational studies of these isomers are discussed in Chapter 5.

The spectral characteristics of asymmetric rotors such as dihydroxyacetone make a definitive interstellar detection quite difficult. While some spectral windows contain multiple emission lines, most contain only one strong line due to the relatively large spacing between adjacent K levels within a given J state. It can be argued that many of the isolated features presented here could arise from other unidentified species or from the excited vibrational state lines of previously detected molecules. This argument is countered by the striking similarity between the observed and simulated spectra shown in Figure 4.6. This degree of coincidental overlap with other hot core species in both rest frequency and intensity is unlikely, but additional observations are clearly warranted.